Effects of surface disorder on EXAFS modeling of metallic clusters

Aaron Yevick and Anatoly I. Frenkel*
Department of Physics, Yeshiva University, 245 Lexington Avenue, New York, New York 10016, USA
(Received 13 February 2010; revised manuscript received 9 March 2010; published 26 March 2010)

Small (1–5 nm) metal clusters may undergo significant surface relaxation under the influence of ligands, adsorbates, and substrate-induced stress. As a result, the nearest-neighbor distance between surface atoms can be reduced by up to 10% relative to those in the cluster core, enhancing the disorder in the interatomic distances. Accordingly, the pair distribution function extracted from EXAFS data under the standard assumption that the distribution function of nearest-neighbor bonds is quasi-Gaussian yields systematic errors. Here we analyze the surface disorder effects with emphasis on their impact on the accuracy of the size and shape determination of nanocatalysts.

DOI: 10.1103/PhysRevB.81.115451 PACS number(s): 61.05.cj, 61.46.Df

I. INTRODUCTION

Nanoparticles in the nanometer range, especially those under 5 nm in size, are attractive as sensors,[1] catalysts,[2] nanoelectronic and optoelectronic devices.[3] Their electronic, structural, magnetic, and optical properties are dramatically different from their bulk counterparts, and are subject of intense investigation. A fundamental challenge, and intrigue, for experimentalists and theorists alike, is to obtain quantitative information about the structural properties of nanoparticles that are not amenable to direct imaging.

In this regard, extended x-ray absorption fine-structure (EXAFS) analysis has proven to be a powerful quantitative tool for structural investigations of nanoclusters almost since the technique was invented in the beginning of the 1970s.[4] In this method, the atom-atom pair distribution information is extracted from the x-ray absorption coefficient data as the x-ray energy is scanned within ca. 1000–1500 eV of the absorbing edge of the atom of interest, as a result of the photoelectron wave interference that modifies the final state of the excited atom. While the data analysis methods and the computer codes that implement them vary, the most common approach to quantifying the pair distribution function is by approximating it as a quasi-Gaussian curve (also known as a cumulant expansion method) that allows to obtain the ensemble-average coordination number as the area under the curve, the average interatomic distance as the centroid, and the mean square disorder in this distance as the standard deviation. This approach, while accurate for materials with small to moderate disorder,[5] fails in systems where the disorder is either large, or the bond length distribution is markedly non-Gaussian.[6,7] In those systems, as was previously shown, Gaussian approximation is inadequate, and EXAFS results obtained by using cumulant expansion are incorrect.

In data modeling, the coordination numbers are normally measured for the first few coordination shells and then compared to different structural motifs. Here results of EXAFS and other complementary techniques are integrated into a single self-consistent model that explains the unique structure, size, shape, and morphology of the nanoparticles.[8–11] Although the synthesis methods are now quite advanced, and can be applied to determine the properties of nanoparticles with narrow size distributions in the size ranges between 1 and 5 nm, no attempts to our knowledge have been performed to examine the analysis strategy and in particular to understand in what circumstances the Gaussian approximation is adequate for nanoparticles. Toward this goal, we here examine strongly disordered systems that are most likely to be incorrectly modeled by conventional methods. In this manner, we can quantify the effect of structural disorder on EXAFS experiments involving nanoclusters.

Nanoclusters belong to a class of systems where enhanced structural disorder is inherent. Indeed, even in free nanoparticles, surface tension[12] induces surface reconstruction,[13] which results in the deviations of the surface atoms from the periodic positions associated with the bulk. Among many possible causes of disorder, and the concomitant change in vibrational properties,[14] are capping ligands,[15] steric effects,[16] crystalline defects (e.g., twins),[17] multiple metastable states,[18,19] and interactions with absorbates.[20,21] In this paper, we limit our analysis to the surface relaxation induced disorder, that is present in numerous systems.

In the following section we introduce the atom-by-atom modeling of EXAFS signal from clusters. Section III applies this procedure to families of clusters with two representative sizes. In these clusters, the surface relaxation is modeled by a radial distortion function that allows modifying the bond length disorder in a controlled manner, one offering the straightforward comparison with available experiments. Model EXAFS signals calculated for distorted clusters were then analyzed by standard methods and the results are given in Sec. IV. Discussion of the results is presented in Sec. V, and finally a summary is given in Sec. VI.

II. MODELING OF BOND LENGTH DISORDER IN CLUSTERS

The edge-step normalized, background subtracted EXAFS signal due to the nearest-neighbor (NN) atoms to an x-ray absorbing atom can be represented as

$$\chi(k) = \int_{r_{\min}}^{r_{\max}} \chi(k,r)\rho(r)dr, \tag{1}$$

where $\rho(r)=dN/dr$ describes the bond length distribution due to static and/or dynamic disorder of the atomic positions.

The limits of integration correspond to the radial spread of NNs within the coordination shell of interest, while dN is the number of NNs to absorbing atoms within the spherical shell of radius r and thickness dr. Each pair (absorber–NN) contributes the following EXAFS signal to Eq. (1),

$$\chi(k,r) = \frac{S_0^2}{kr^2} f(k) e^{-2r/\lambda(k)} \sin[2kr + \delta(k)], \tag{2}$$

where S_0^2 is the passive electron reduction factor, and functions $f(k)$, $\delta(k)$, and $\lambda(k)$ are the scattering amplitude, phase, and mean free-path, respectively. The EXAFS signal contains ensemble-average local structural characteristics, such as the coordination number (N), mean bond length (R), and the mean square disorder (σ^2) of the bond lengths that can be defined via $\rho(r)$ as

$$N = \int_{r_{\min}}^{r_{\max}} \rho(r) dr, \quad R = \int_{r_{\min}}^{r_{\max}} r\rho(r) dr,$$

$$\sigma^2 = \int_{r_{\min}}^{r_{\max}} (r - R)^2 \rho(r) dr. \tag{3}$$

In strongly disordered systems, $\rho(r)$ may be broad or asymmetric and therefore not known *a priori*. Therefore the above quantities cannot be reliably extracted from EXAFS analysis. In systems with small to moderate disorder, both $\rho(r)$ and the effective radial distribution function $g(r) = \rho(r)/r^2$ can be approximated as quasi-Gaussian distributions. In that case, $\rho(r)$ in Eq. (1) is replaced by its cumulant expansion[22] that allows to represent theoretical EXAFS signal with just a small number of leading cumulants that are simply expressed through the quantities N, R, and σ^2,

$$\chi(k) = \frac{NS_0^2}{kr^2} f(k) e^{-2k^2\sigma^2} e^{-[2r/\lambda(k)]} \sin\left(2kr - \frac{4}{3}\sigma^{(3)}k^3 + \delta(k)\right). \tag{4}$$

Equation (4) contains also a third cumulant, $\sigma^{(3)}$, that describes the asymmetry of $\rho(r)$. In systems with non-Gaussian disorder, however, this method breaks down, in part, due to the large number of cumulants required to fit $\rho(r)$. Among such systems, the most notable examples are strongly disordered[23] and amorphous[7,24] solids where the asymmetry of $\rho(r)$ results in the underestimation of the coordination numbers (N) and EXAFS Debye-Waller factors (σ^2) if analyzed by Eq. (4). A useful alternative to the Gaussian approximation is the splice method,[6] where the radial distribution function is extracted from the data by a back Fourier transform. This procedure, however, is somewhat model-dependent, as it relies on the cumulant expansion of the data at the low k region.

Nanoparticles represent an interesting class of systems with mean squared bond length disorder σ^2 contributed by both static (σ_s^2) and dynamic (σ_d^2) components: $\sigma^2 = \sigma_s^2 + \sigma_d^2$. The static contribution can have numerous causes: due to the amorphous nature of sub-nm particles,[25] presence of multiple twins, or due to the surface-induced disorder, *vide supra*. The latter is commonly associated with surface tension, which causes the surface atoms to relax inward.[13] Because of the short range and the inherent asymmetry of such deformations the radial distribution functions are expected to be strongly non-Gaussian. In the next sections we examine the accuracy of the cumulant expansion in modeling such distributions, by first generating theoretical EXAFS signals of distorted clusters and then employing conventional methods to analyze them.

III. SIMULATING SURFACE TENSION BY RADIAL DISTORTION MODEL

We modeled EXAFS data in computer-generated Au clusters with 147 and 923 atoms, representing two important sizes with 1.7 and 3.4 nm diameters. The undistorted clusters are modeled as perfect cuboctahedra with nearest-neighbor distances of 2.87 Å (corresponding to interatomic distances in bulk Au). To simulate surface tension effects we multiplied the distance of each atom from the center of the cluster by a radial distortion function. We expect that the outer atoms are more affected by surface tension-induced strain than the inner atoms,[13] and accordingly employed the empirical distortion function

$$f(r) = A + (1 - A)\exp(Cr), \quad \text{where } C = \frac{1}{R}\ln\left(\frac{B - A}{1 - A}\right). \tag{5}$$

This function satisfies the conditions: $f(0) = 1$, $f(R) = B \leq 1$ at the cluster center and periphery, respectively. The parameter A yields the curvature of the distortion curve as shown in Fig. 1. In order to simulate a range of possible distortions, we considered four different values of A: 1.05, 1.001, 1.0001, and 1.00001, corresponding to uniformly and non-uniformly distorted structures [Fig. 1(a)]. We approximated B by 0.95, which agrees well with physically reasonable bond length truncation effects in small clusters. The different distortion functions correspond to different distributions of the 1NN distances and simulate the radial relaxation of the surface tension from the outer layers of the cluster inward. These can therefore be directly compared to available experimental data. For example, $f(r)$ with $A = 1.000\,01$ and $B = 0.95$ generates very similar bond lengths to those obtained by Huang *et al.*[26] by modeling their electron diffraction data of Au clusters containing 1050 atoms [Fig. 1(b)].

For all distorted clusters we used the known x, y, z coordinates of all atoms to approximate radial distribution function $\rho(r)$ by a frequency distribution histogram $\rho(r_i)$, in which histogram bin index $i = 1, 2, \ldots n$. The bin size $\Delta r_i = 0.005$ Å is centered around the bond length r_i. Following Eqs. (1) and (2), where we replaced integration by summation over the range of distances corresponding to the first coordination shell around absorbing atoms, we constructed EXAFS "data" corresponding to the 1NN contribution only,

$$\chi(k) = \frac{S_0^2}{k} f(k) \sum_{i=1}^{n} \frac{\rho(r_i)\Delta r_i}{r_i^2} e^{-[2r_i/\lambda(k)]} \sin[2kr_i + \delta(k)]. \tag{6}$$

$f(k)$, $\delta(k)$, and $\lambda(k)$ were calculated by FEFF6 code[27] for central atoms in the Au clusters and were held the same for

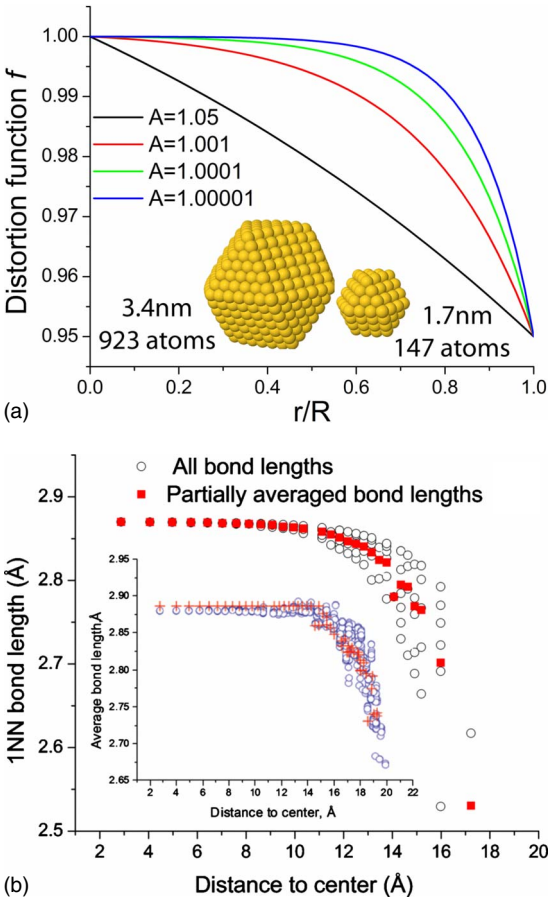

FIG. 1. (Color online) (a) Different distortion functions corresponding to $B=0.95$. Two clusters of different sizes are shown, both distorted with $A=1.000\,01$, $B=0.95$. (b) Bond lengths distributions (ones obtained by averaging over the 1NN coordination shells of all atoms at a given distance from the center of the cluster, as well as over all bond lengths emerging from such atoms), calculated in the 923 atom Au clusters, distorted using $A=1.000\,01$ and $B=0.95$. Inset corresponds to the Fig. 3 from Ref. 26 (Adapted by permission from Macmillan Publishers Ltd) obtained by electron diffraction data modeling and molecular dynamics simulations for the 1050-atom Au cluster.

all atoms in the clusters. Such atom-to-atom transferability was validated by testing different absorbing sites within the clusters (e.g., center vs surface). We found that, within the accuracy of FEFF6 code, these functions were effectively independent of the site location. This method of constructing XAFS data can be employed for any coordination shell provided an appropriate histogram is constructed. However, we simulated the data only for the first coordination shell, as this shell yields the most useful information.

All data generated with Eq. (6) were analyzed in identical conditions, using FEFF6 theory for the Au-Au 1NN contribution that was fit to the data using Artemis software.[28] The k range and r range in the fits were from 2 to 18 Å^{-1} and from 1.51 to 3.36 Å, respectively, with small variations between different data sets, corresponding to a total number of relevant independent data points equal to 18. There were five variables in the fit done using quasi-Gaussian approximation [Eq. (4)], namely, the apparent coordination number N, the

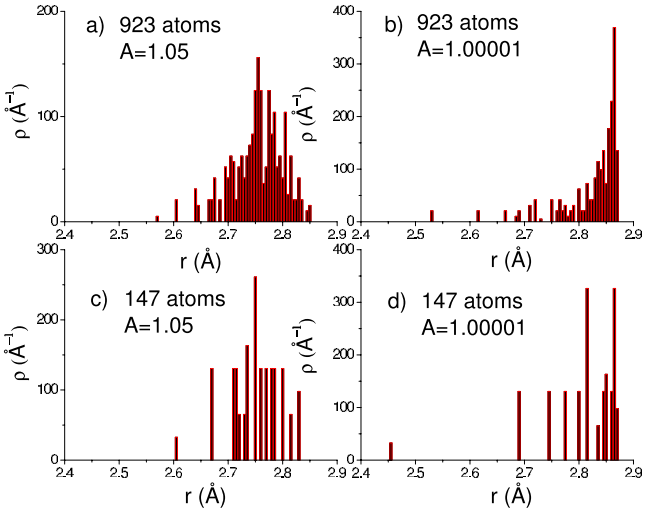

FIG. 2. (Color online) The first nearest-neighbor radial distribution functions for the 147 and 923 atom clusters with $A=1.05$ (left figures) and 1.000 01 (right figures).

distance correction ΔR, σ^2, the energy origin correction ΔE_0, and the third cumulant $\sigma^{(3)}$. Through this analysis we could compare the actual and the apparent structural characteristics of the distorted clusters. Finally, the EXAFS signals for the corresponding undistorted clusters of each size were generated using the same procedure [with $n=1$ in Eq. (6)] and analyzed in the same manner as the distorted data, to calibrate accuracy of our approach.

IV. RESULTS

Figure 2 shows representative histograms $\rho(r_i)$ for differently distorted clusters of the two sizes of interest. Due to the nature of the distortion represented by $A=1.05$, which corresponds to the long range elastic strain affecting most of the atoms of the cluster, the distributions [Figs. 2(a) and 2(c)] are broad and symmetric. In contrast, other distortion parameters (most notably, $A=1.00001$, which best matches the results of Huang *et al.*,[26]) generate strongly distorted, non-Gaussian distributions [Figs. 2(b) and 2(d)].

We simulated EXAFS data for all distribution functions. The data for undistorted clusters, together with clusters with different degrees of radial distortion, are shown in k space and r space in Fig. 3. By visually examining the data, the effects of distortions appear to be similar to what is expected from the simple Debye-Waller factor effect and from the average 1NN distance change between different clusters. The former effect reduces oscillation intensity in the large k region, while leaving it relatively unaffected in the low k region, i.e., just what we observe in the data behavior for distorted clusters. The latter effect would cause the oscillation frequency (in k space) to decrease, and the peak position (in r space) to shift to the left. This behavior is most pronounced for

$A=1.05$, which is associated with bulk-like bond length changes compared to the other distortion functions.

The data and the corresponding best fits for the 147 atom clusters are shown in Fig. 4. The numerical results for the

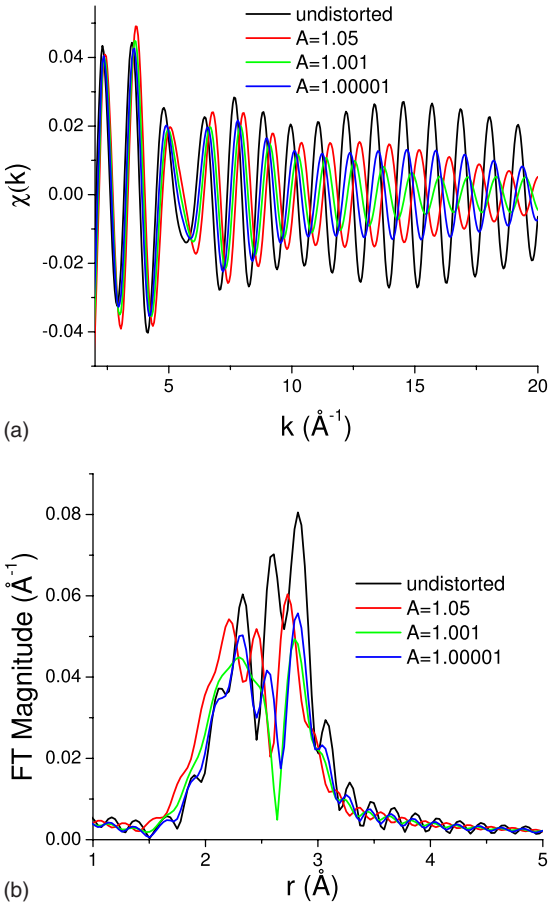

FIG. 3. (Color online) *k*-space (a) and *r*-space (b) EXAFS data constructed using radial distribution function method for the 147 atom Au clusters.

EXAFS data analysis of clusters of different sizes, generated with different distortion functions, are tabulated in Tables I and II. The 1NN coordination numbers associated with the structure and geometry of the undistorted clusters are 10.35 (for 923 atoms) and 8.98 (for 147 atoms). To match these values through fits to their respective data required the addition of a constant scaling factor equal to 1.0095 to the right side of Eq. (6) for all our distorted cluster analyses. This 1% amplitude correction, which is a cumulative artifact of interpolation effects, and somewhat arbitrary Hanning window parameters used in the fits, has a negligible impact on the results below.

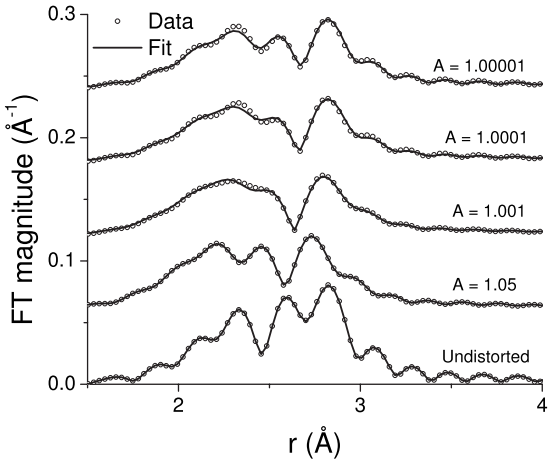

FIG. 4. Data and fits (in *r* space) for the distorted 147 atom clusters.

As evident from the data behavior and bond length distribution histograms presented above, our fitting analysis confirmed that for $A=1.05$ quasi-Gaussian approximation is reliable. The best fit values for the adjustable variables (Tables I and II) were found to be in a good agreement with those independently calculated for the known cluster structures. The results obtained for those distortion functions that generated more asymmetric distributions, particularly for *A* values of 1.0001 and 1.000 01 (see also Fig. 2), are however in marked disagreement with the actual values for the both types of clusters investigated. The actual values for these clusters sizes presented in Tables I and II were calculated using known radial distributions Eqs. (3). The best fit values of the third cumulants were consistent with zero, within the error bars, and are therefore not reported.

V. DISCUSSION

As Tables I and II show, the coordination numbers obtained by the fit to the most distorted configurations are underestimated by 8% for both cluster sizes. The nearest-neighbor distances are by 0.01 Å longer than the actual values for the most asymmetric configurations, and the mean square disorders in the bond lengths are consistently underestimated. Figure 5 demonstrates the gradual reduction in the best fit coordination numbers as the asymmetry of the distortion function increases, for both cluster sizes we investigated.

As noted in Sec. I, the nearest-neighbor coordination numbers are often a primary method of obtaining the information about the particle size and shape, especially if experiments are done *in situ*, during reaction conditions. Indeed, EXAFS is unique in its ability to monitor real-time, local structural changes in the samples under high temperature and gas pressure, during chemical reactions, where independent knowledge of the structure by other methods is difficult to obtain. For example, recently, Newton *et al.* performed highly original *in situ*, combined EXAFS/infrared spectroscopy experiments and recorded cyclic changes of the intensity of EXAFS oscillations in response to CO/NO cycling.[29] They subsequently interpreted these results in terms of the cyclic changes of the Pd-Pd coordination numbers which, in turn, suggested that the particles were undergoing cyclic changes in their size and shape. Our results indicate that an alternative explanation can be advanced, where no changes in the particle size or shape occurs as a result of CO/NO cycling. Instead, these two types of adsorbates disorder the surface differently: NO does it more strongly than CO, resulting, as we showed, in the greater reduction of the apparent coordination number (Fig. 5).

A second example of an apparent reduction in the coordination number caused by the strong surface reconstruction relative to the cluster core is recent work by Sanchez *et al.*[30]

TABLE I. Best fit results for the 923 atom Au cluster.

	N		ΔR (Å)		σ^2 [Å^2($\times 10^4$)]		ΔE (eV)	
Distortion parameter A	Data	Fit	Data	Fit	Data	Fit	Data	Fit
Undistorted	10.35	10.35(6)	0	0.0019(7)	0	−1.7(2)	0	0.04(4)
1.05	10.35	10.29(3)	−0.1161	−0.1151(5)	22	17.5(2)	0	−0.50(3)
1.001	10.35	9.7(2)	−0.081	−0.072(3)	43	18.9(1)	0	−0.1(1)
1.0001	10.35	9.5(2)	−0.062	−0.048(3)	46	13(1)	0	0.1(2)
1.00001	10.35	9.6(2)	−0.047	−0.033(2)	44	8.6(8)	0	0.2(1)

Here the coordination numbers of Pt nanoparticles on $\gamma-Al_2O_3$ and Pt/C supports have their Pt-Pt coordination numbers decreased in He environment compared to H_2 for all sizes studied (from 0.9 to 2.9 nm), with the exception of the 1.8 nm Pt/C particles for which the numbers were identical, within experimental uncertainties. As shown in that, and many previous EXAFS studies,[31–33] Pt nanoparticles in hydrogen are relatively ordered (compared to an inert environment or vacuum), and possess relatively long Pt-Pt distances that are close to their bulk values. Wang and Johnson attributed such ordering and the bond length increase to the stabilization of the truncated cuboctahedral structure resulting from H passivation.[25] Our simulations however demonstrate that surface ordering could explain the apparent reduction in the coordination number of Pt-Pt neighbors when hydrogen is replaced by helium in the sample chamber, due to the enhanced disorder of the Pt nanoparticle surface after hydrogen desorption.

We note that the effects of enhanced surface disorder may be partly responsible for the often reported reduction in the EXAFS-determined coordination numbers compared to those obtained by independent techniques.[34] Indeed, the reduction of the coordination numbers from 10.35 to 9.6 (Table I) corresponds to a change in the number of atoms in the cluster from 923 to 309 assuming a cuboctahedral cluster series,[35] i.e., the cluster diameter decreases from 3.4 nm to 2.3 nm (Fig. 5). Of course, such a change could be an artifact of the EXAFS analysis, and the actual size of the cluster is 3.4 nm, while the only reason for the "reduction" is the inadequacy of the quasi-Gaussian approximation for the pair distribution function used in the analysis, as our work demonstrates.

In this work we deliberately focused on the static, temperature-independent disorder in the atomic positions, ignoring the contribution of thermal disorder. This approach allows us to model many clusters quickly and efficiently. Vibrational contributions to $\rho(r)$ are accessible from, e.g., molecular dynamics simulation. For low temperatures, thermal contribution to $\rho(r)$ may be modeled, to a good approximation, as a quasi-Gaussian with just a few leading cumulants.[36] That means, the contribution of the thermal disorder to the total $\rho(r)$ will be reduced to broadening it—by an amount that can be estimated by EXAFS data modeling, which is beyond the scope of this work.

Finally, we address two challenges revealed in this work for structural analysis of metal nanoparticles by EXAFS. The first challenge is how to uncover the enhanced disorder of the type described here, one underestimated by most common analysis methods, and the second challenge is how to correct for it. To observe the surface disorder effects, electron microscopy and diffraction are powerful and efficient tools, as shown in Ref. 26. Cluster size and shape determination can be done by combining high resolution and atom-counting methods of electron microscopy.[37] Accounting for thermal effects (in order to break the correlation between the effects of the structural disorder and the coordination number) can be accomplished by *in situ* measurements under different temperatures. Finally, the sensitivity to these effects can be greatly enhanced with the access to very well defined, nearly monodisperse samples (since the coordination numbers, bond distances, and their disorder are strongly size-dependent for particles under 5 nm in size).

For the problem described here, i.e., when the near-surface bond length contraction is responsible for the cluster-average bond length disorder and the consequent reduction in the apparent coordination number, one remedy may be to analyze the same system under different adsorbates, ones

TABLE II. Best fit results for the 147 atom Au cluster.

	N		ΔR (Å)		σ^2 [Å^2($\times 10^4$)]		ΔE (eV)	
Distortion parameter A	Data	Fit	Data	Fit	Data	Fit	Data	Fit
Undistorted	8.98	8.98(6)	0	0.0020(7)	0	−1.7(2)	0	0.05(5)
1.05	8.98	8.94(3)	−0.1198	−0.1185(4)	20	16.0(2)	0	−0.51(2)
1.001	8.98	8.9(1)	−0.089	−0.087(3)	41	29(1)	0	−0.4(1)
1.0001	8.98	8.5(2)	−0.071	−0.067(4)	48	23(2)	0	−0.2(2)
1.00001	8.98	8.3(2)	−0.058	−0.047(4)	49	14(1)	0	0.0(2)

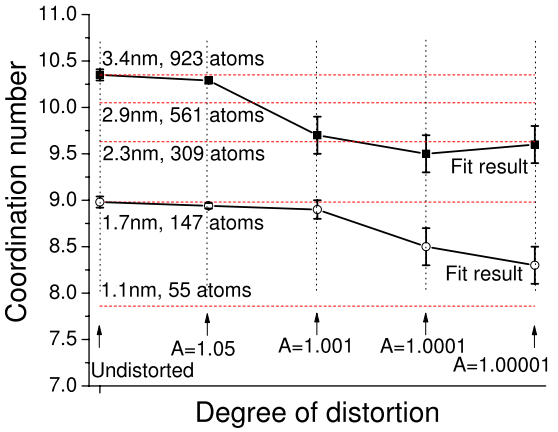

FIG. 5. (Color online) Coordination numbers of the first nearest neighbors obtained using quasi-Gaussian approximation by FEFF6 fit to the data generated for model Au clusters of 147 and 923 atoms with different radial distortions. Best fit results are shown with symbols, while the model coordination numbers are shown as horizontal dashed lines. The solid lines are the guides to the eye.

that modify the strength of metal-metal bonds near the surface. For example, as shown in many previous studies, when the surface is passivated by H_2 or CO, the clusters can be better approximated by periodic atomic ensembles. Such systems are good benchmark tests for size and shape determination by multiple-scattering methods of EXAFS analysis employing quasi-Gaussian approximation for bond length disorder, appropriate in such cases. For more distorted clusters, where enhanced surface disorder is induced by the *in situ* changes in the metal-adsorbate interaction, the modeling strategy proposed in this work, one utilizing parameters A and B for the radial distortion function, can be used on par with other methods accounting for possible changes in the size and shape of the clusters. This approach can be easily extended to modeling other types of distortions, e.g., interfacial disorder near the substrate,[38] or ligand-induced tangential disorder,[39] or the combination of these and other effects.

VI. SUMMARY

In this work we investigated effects of structural disorder specific to nanoparticles undergoing strong surface reconstructions on their EXAFS analysis results. We estimate the errors in the coordination numbers, bond lengths, and their mean square disorder values assuming structural models whose distortion parameters fit well to the available experimental data. We demonstrate that enhanced surface disorder in metal nanoparticles, in the size range under 5 nm, if unaccounted for, may result in the significant underestimation of particle size and overestimation of the nearest neighbor distances.

ACKNOWLEDGMENTS

We acknowledge the support of this work by the U.S. DOE under Grants No. DE-FG02-03ER15476 and DE-FG02-05ER15688. The authors are grateful to B. Ravel for useful discussions.

*Corresponding author; anatoly.frenkel@yu.edu

[1] A. H. Shipway, E. Katz, and I. Willner, ChemPhysChem **1**, 18 (2000).
[2] B. F. G. Johnson, Top. Catal. **24**, 147 (2003).
[3] E. K. Athanassiou, R. N. Grass, and W. J. Stark, Nanotechnology **17**, 1668 (2006).
[4] F. Lytle, D. Sayers, and E. A. Stern, Phys. Rev. B **11**, 4825 (1975).
[5] E. D. Crozier, J. J. Rehr, and R. Ingalls, *X-ray absorption. Principles, Applications, Techniques of EXAFS, SEXAFS, and XANES* (Wiley, New York, 1988), Chap. 9.
[6] E. A. Stern, Y. Ma, O. Hanske-Petitpierre, and C. E. Bouldin, Phys. Rev. B **46**, 687 (1992).
[7] A. Frenkel, E. A. Stern, A. Voronel, A. Rubshtein, Y. Ben-Ezra, and V. Fleurov, Phys. Rev. B **54**, 884 (1996).
[8] A. I. Frenkel, J. Synchrotron Radiat. **6**, 293 (1999).
[9] A. I. Frenkel, C. W. Hills, and R. G. Nuzzo, J. Phys. Chem. B **105**, 12689 (2001).
[10] L. D. Menard, H. Xu, S.-P. Gao, R. D. Twesten, A. S. Harper, Y. Song, G. Wang, A. D. Douglas, J. C. Yang, A. I. Frenkel, R. W. Murray, and R. G. Nuzzo, J. Phys. Chem. B **110**, 14564 (2006).
[11] A. M. Karim, V. Prasad, W. W. Lonergan, A. I. Frenkel, J. G. Chen, and D. G. Vlachos, J. Am. Chem. Soc. **131**, 12230 (2009).
[12] J. S. Vermaak, C. W. Mays, and D. Kuhlmann-Wilsdorf, Surf. Sci. **12**, 128 (1968).
[13] R. J. Needs and M. Mansfield, J. Phys.: Condens. Matter **1**, 7555 (1989).
[14] B. Gilbert, F. Huang, H. Zhang, G. A. Waychunas, and J. F. Banfield, Science **305**, 651 (2004).
[15] A. C. Carter, C. E. Bouldin, K. M. Kemner, M. I. Bell, J. C. Woicik, and S. A. Majetich, Phys. Rev. B **55**, 13822 (1997).
[16] J.-J. Shiang, A. V. Kadavanich, R. K. Grubbs, and A. P. Alivasatos, J. Phys. Chem. **99**, 17417 (1995).
[17] B. S. Xu and S.-I. Tanaka, Nanostruct. Mater. **8**, 1131 (1997).
[18] L. L. Wang and D. D. Johnson, Phys. Rev. B **75**, 235405 (2007).
[19] A. P. Chernyshev, Mater. Chem. Phys. **112**, 226 (2008).
[20] G. A. Somorjai, *Introduction to Surface Chemistry and Catalysis* (Wiley, New York, 1994).
[21] G. Rupprechter and H.-J. Freund, Top. Catal. **14**, 3 (2000).
[22] E. Sevillano, H. Meuth, and J. J. Rehr, Phys. Rev. B **20**, 4908 (1979).
[23] C. E. Bouldin and E. A. Stern, in *EXAFS Studies of Amorphous Semiconductors, EXAFS and Near EdgeStructure III*, edited by K. O. Hodgson, B. Hedman, and J. E. Penner-Hahn (Springer-Verlag, Berlin, 1984), p. 273.
[24] V. L. Aksenov, M. V. Koval'chik, A. Yu. Kuz'min, Yu. Purans, and S. I. Tyutyunnikov, Crystallogr. Rep. **51**, 908 (2006).
[25] L. L. Wang and D. D. Johnson, J. Am. Chem. Soc. **129**, 3658 (2007).

[26] W. M. Huang, R. Sun, J. Tao, L. D. Menard, R. G. Nuzzo, and J. M. Zuo, Nature Mater. **7**, 308 (2008).
[27] S. I. Zabinsky, J. J. Rehr, A. Ankudinov, R. C. Albers, and M. J. Eller, Phys. Rev. B **52**, 2995 (1995).
[28] B. Ravel and M. Newville, J. Synchrotron Radiat. **12**, 537 (2005).
[29] M. A. Newton, C. Belver-Coldeira, A. Martínez-Arias, and M. Fernández-García, Nature Mater. **6**, 528 (2007).
[30] S. I. Sanchez, L. D. Menard, A. Bram, J. H. Kang, M. W. Small, R. G. Nuzzo, and A. I. Frenkel, J. Am. Chem. Soc. **131**, 7040 (2009).
[31] M. K. Oudenhuijzen, J. A. van Bokhoven, D. E. Ramaker, and D. C. Koningsberger, J. Phys. Chem. B **108**, 20247 (2004).
[32] M. K. Oudenhuijzen, J. A. van Bokhoven, J. T. Miller, D. E. Ramaker, and D. C. Koningsberger, J. Am. Chem. Soc. **127**, 1530 (2005).
[33] D. C. Koningsberger and M. K. Oudenhuijzen, J. de Graaf, J. A. van Bokhoven, D. E. Ramaker, J. Catal. **216**, 178 (2003).
[34] S. Calvin, M. M. Miller, R. Goswami, S.-F. Cheng, S. P. Mulvaney, L. J. Whitman, and V. G. Harris, J. Appl. Phys. **778**, 94 (2003).
[35] D. Glasner and A. I. Frenkel, AIP Conf. Proc. **882**, 746 (2007).
[36] A. I. Frenkel and J. J. Rehr, Phys. Rev. B **48**, 585 (1993).
[37] A. I. Frenkel, J. C. Yang, D. D. Johnson, and R. G. Nuzzo, in *Encyclopedia of Complexity and Systems Science*, edited by R. Meyers (Springer, New York, 2009), Vol. N, pp. 5889–5912.
[38] L.-L. Wang, S. V. Khare, D. D. Johnson, A. A. Rockett, V. Chirita, A. I. Frenkel, N. H. Mack, and R. G. Nuzzo, J. Am. Chem. Soc. **128**, 131 (2006).
[39] O. Guliamov, A. I. Frenkel, L. D. Menard, R. G. Nuzzo, and L. Kronik, J. Am. Chem. Soc. **129**, 10978 (2007).